JOURNAL OF MATERIALS SCIENCE 19 (1984) 1–23

Review
Semiconducting transparent thin films: their properties and applications

A. L. DAWAR, J. C. JOSHI
Defence Science Centre, Metcalfe House, Delhi 110054, India

The present state of the art of transparent, electrically conducting films, with special reference to In_2O_3, SnO_2 and Cd_2SnO_4, has been reviewed. Various production techniques currently in use, and typical parameters used in the processes have been discussed in detail. Electrical and optical properties of these films have been reported as a function of various parameters, e.g. substrate temperature, doping, oxygen pressure, etc. Finally, the applications of these films in research and industry have been discussed in detail.

1. Introduction

Studies of transparent and highly conducting semiconductor films have attracted the interest of many research workers because of their wide applications in both industry and research. Important applications can be classified in four major groups.

1.1. Transparent heat reflecting films

These films are used for heat insulation where unhindered light transmission is required. The films on the one hand efficiently reflect broadband infrared heat radiation in a manner similar to highly conductive metal-like materials; and on the other hand they transmit light effectively in the visible region as if they were insulators. Such spectrally selective films have wide applications in solar thermal energy conversion, solar photovoltaic conversion, solar heating, window insulation and thermal insulation in lamps.

1.2. Heterojunction solar cells

Heterojunction solar cells with an integral conducting transparent layer offer the possibility of fabrication of low cost solar cells with performance characteristics suitable for large scale terrestial applications. The method of production of these conducting transparent films is consistent with high yield and fast throughput processing. It also involves low substrate temperatures as compared to diffusion processes, avoiding the chances of degradation of semiconductor minority carrier properties, that are important in a solar energy conversion device. The conducting transparent film permits the transmission of solar radiation directly to the active region with little or no attenuation. These solar cells thus have improved sensitivity in the high-photon-energy portion of the solar spectrum. In addition, the conducting transparent film can serve simultaneously as a low-resistance contact to the junction and as an anti-reflection coating of the active region. Solar cells utilizing these transparent conducting coatings are now being fabricated widely, e.g. SnO_2/Si, In_2O_3/Si, ITO/Si, ITO/SiO_x/Si.

1.3. Gas sensors

Unlike metal films whose conduction modulation by gas adsorption is small and related to changes in surface scattering, the conductance changes in semiconductor materials are large and are caused primarily by changes in carrier concentration due to charge exchange with the species adsorbed from the gas phase. The electron concentration in semiconductor sensors can vary in the conduction band approximately linearly with pressure, over a range of up to eight decades, while variations in the carrier mobility are generally small. It is this large and reversible variation in conductance with active gas pressure that has made semiconductor materials attractive for the fabrication of gas sensing electronic transducers. The semiconducting properties of the transparent conducting films have been

0022–2461/84 $03.00 + .12

exploited for use of these films in the sensing of various gases, e.g. carbon monoxide, propane and hydrogen.

1.4. Protective coatings

It has been reported [1] recently that the application of a metallic oxide coating to glass containers reduces appreciably the coefficient of friction of the glass surfaces, facilitating the movement of containers through high speed fitting lines. It has now become common practice to apply these metallic oxide coatings to glass containers immediately after forging. The subsequent application of an organic lubricant to the cooled and annealed container gives a highly desirable change to the glass surface, particularly with respect to the abrasion resistance and lubricity.

1.5. Other applications

In addition to these main applications, these transparent conducting films are now being widely used in a variety of other applications, such as the production of heating layers protecting vehicle windscreens from freezing and misting over [2], light-transmitting electrodes in the development of optoelectronic devices [3, 4]; laser-damage resistant coatings in high power laser technology [5]; the photocathode in photoelectrochemical cells [6]; antistatic surface layers on temperature control coatings in orbiting satellites [7]; and surface layers in electroluminescent applications [8].

A large number of materials can be used for these applications, e.g. In_2O_3, SnO_2, $CdSnO_3$, Cd_2SnO_4, $CdIn_2O_4$ and In_2TeO_6. Some of the important properties of these materials are shown in Table I. So far, most of the research on the fabrication of transparent coatings has been restricted to oxides of tin, indium and a combination of their oxides because of the low cost. Recently some work has been reported on the fabrications of $CdSnO_4$ coatings, but no applications have yet been reported. SnO_2, In_2O_3 and Cd_2SnO_4 are n-type degenerate semiconductors with low resistivity ($\sim 10^{-2}$ to 10^{-4} ohm cm) and a wide band gap (2.3 to 4.6 eV) which produces a high transparency in the visible spectrum. Good conductivity in these materials is obtained by introducing carriers in one of two ways. Oxygen deficiency may be created by heating in a slightly reducing atmosphere. Such a process is reversible and the carriers so created may be removed by heating in air or oxygen at relatively low temperatures (500 to 1000° C). The other method involves chemical doping, for example by fluorine in the case of SnO_2 or by tin in In_2O_3. The F^- anion substitutes for an O^{2-} anion in the lattice, creating a donor level in the band gap [9]. Similarly the substitution of an In^{3+} cation by an Sn^{4+} cation leads to a donor level in the band gap [10]. The method of chemical doping is considered to be better from the practical viewpoint since it has the advantage that the resistivities are relatively unaffected by heating or atmospheric exposures.

The need for coatings which have both low resistivities and high transparency in the visible region has led to the development of various deposition techniques such as r.f. sputtering and d.c. sputtering of oxide targets; reactive sputtering, in the presence of oxygen, of indium, tin, indium–tin or tin–cadmium alloy; ion beam sputtering; ion plating; evaporation of oxide materials; reactive evaporation of metals in the presence of oxygen plasma-assisted reactive evaporation; flash evaporation of oxidic powders; chemical vapour deposition; and hydrolysis or spray. Each of these processes has its own merits and demerits. For example, sputtering techniques allow the fabrication of high quality films but they have high equipment cost and a relatively low production rate, and spray techniques are very cheap but the films produced are not consistent.

The results reported by different workers using different techniques vary significantly. There is a wide diversity in the optimized dopant concentration for the best quality films. This is probably because of differences in the deposition par-

TABLE I Some properties of transparent conducting oxides at room temperature

Serial number	Compound	Structure-type	Cell dimensions (nm)			Resistivity (ohm cm)	Band gap (eV)
			a	*b*	*c*		
1	In_2O_3	Tl_2O_3 (cubic)	1.0117	–	–	10^{-2}–10^{-4}	3.7–4.4
2	SnO_2	Rutile	0.4737	–	0.31861	10^{-2}–10^{-4}	3.9–4.6
3	Cd_2SnO_4	Sr_2PbO_4	0.5568	0.9887	0.3192	10^{-3}–10^{-4}	2.34–2.76
4	In_2TeO_6	Na_2SiF_6	0.8882	–	0.4821	$\sim 10^{-2}$	–
5	$CdIn_2O_4$	Spinel	0.9167	–	–	$\sim 10^{-4}$	–

ameters and the purity of the elements. Though a lot of work has been done to understand the conduction mechanism in these films, conclusive evidence is still lacking. Bosnell and Waghorne [11] have combined the X-ray, Auger and ESCA results on indium–tin oxide films to resolve differences of results. They concluded that intermediate tin oxide states such as Sn_3O_4 are present and anion vacancies are generated by such suboxides of SnO_2, which act as a dopant in In_2O_3. Fan and co-workers [12, 13], on the other hand, stated that interstitial tin is mainly responsible for the conduction in SnO_2 films. These interstitial atoms give rise to a shallow donor impurity level (0.03 eV).

The aim of the present article is to review the present state of the art of transparent, electrically conducting films, with special reference to doped and undoped In_2O_3, SnO_2, indium–tin oxide and cadmium stannate. Various production techniques currently in use, and typical parameters used in the processes are reported in detail. The electrical and optical properties of these films are discussed as a function of various parameters, such as doping, temperature, oxygen pressure, etc. Finally, applications of these films in devices are reported. Optimization of various parameters for different applications are also discussed.

2. Fabrication techniques

Many methods have been tried out to fabricate coatings of the oxide materials. Reviews of earlier work are available in [14–16]. There follows below a brief account of the methods used, particularly during the last five years, in the preparation of such coatings and also the typical parameters used.

2.1. Chemical vapour deposition (CVD)

Chemical vapour deposition is based on the use of volatile organometallic compounds of tin, indium, cadmium, antimony, etc. The deposition set-up commonly used is shown in Fig. 1. The apparatus consists mainly of a rotating hot-plate reactor. The size of the substrate is normally small in order to produce uniform coatings. The temperature of the hot-plate can be adjusted. The organometallic

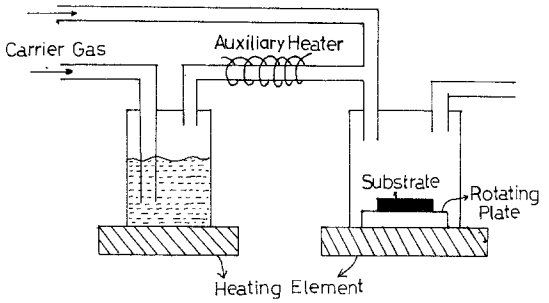

Figure 1 Basic set-up for the deposition of thin transparent conducting films using CVD technique.

compounds are kept in a separate container, which is surrounded by a liquid bath, the temperature of which can be controlled. There is an auxiliary heater to prevent vapours from condensing in the delivery tube. The rates of flow of the gas and of the reactant gas are adjustable. Many workers [17–33] have reported the growth of conducting transparent films using this technique. Kane *et al.* [25] have grown tin oxide films using dibutyl tin diacetate as the organometallic compound, nitrogen as the carrier gas and oxygen as the reactant gas. The substrate was kept at a temperature of about 420° C. These authors also attempted to grow films under wet CVD conditions. Nitrogen and oxygen of the desired ratio were bubbled through the distilled water before being passed to the reaction chamber. It was observed that the presence of water vapours improved both the electrical and optical properties of the films. The best films were reported to have a sheet resistivity of ~ 544 ohm $\square^{-1}$ * and average transmission of $\sim 90\%$. Antimony-doped SnO_2 films were also fabricated [26] under similar conditions. Antimony was added in the form of antimony pentachloride, which was kept in liquid form in a separate container and its vapour was transported into the reaction chamber using nitrogen as the carrier gas. The ratio of the antimony-to-tin was controlled by adjusting the flow rate of the carrier gas. Baliga and Gandhi [27] have used this technique to grow undoped and doped SnO_2 films by using tetramethyl tin as the base organometallic compound, argon as the carrier gas and the oxygen as the reactant gas. The rate of flow of the carrier gas was $2.01\,m^{-1}$. Phosphorus was

*The resistance of a rectangularly shaped section of the film is given by $R = (\rho/t)(l/l_e)$ where ρ is the resistivity (in ohm cm), t is the thickness and l and l_e are the length and width of the film. If $l = l_e$, i.e. the film has a square shape irrespective of the dimensions, $R = \rho/t = R_s$. This R_s, i.e. the resistance of one square unit of the film, depends only on the resistivity and thickness of the film, and is called the sheet resistivity of the film.

added to the films by simultaneously passing a controlled quantity of phosphine gas. The optimum ratio of PH_3/TMT was observed to be 0.01. The best films were reported to have a conductivity of 200 $ohm^{-1}cm^{-1}$ and a transmission of ~90% in the visible range. Arsenic-doped SnO_2 films were also fabricated [28] using the same technique and doping was accomplished by introducing arsine gas in argon. The flow rates of arsine/argon and TMT/argon were adjusted in order to vary the arsenic concentration in the films. The doping with arsenic was observed, however, not to be as effective as with phosphorus. Gandhi *et al.* [29] have recently extended their work to grow SnO_2 films by adopting the CVD technique to use radio frequency (r.f.) plasma-activated oxygen as the reactant. The main advantage of this technique is that it allows the growth of high quality films at room temperature. The reactor chamber was a vertical cylinder of diameter 10.5 cm, and r.f. excitation at a frequency of 3.75 MHz was used to create the oxygen plasma in this system. The total system pressure in the reactor chamber was about 0.5 torr. Tabata *et al.* [30] have modified the usual CVD technique to grow SnO_2 and In_2O_3 films. In this technique, a high speed directed stream of inactive gas carried and deposited reacting materials on to the sample surface. The gas stream was directed at an optimum angle to the specimen surface and afterwards removed through an exhaust. The effect of using such a geometry was almost to eliminate the haze which otherwise tends to be present in the films grown using CVD. Blocher [31] and Kalbskopf [32] have further extended this technique to deposit continuously transparent conducting coatings onto glass ribbons. They obtained very uniform coatings.

2.2. Spraying techniques

Spraying methods are based on the pyrolytic decomposition of tin, indium or cadmium compounds dissolved in a liquid mixture when it is sprayed onto a previously heated substrate. Many variants have been tried to grow these films but the basic technique used by all the workers is similar to that shown in Fig. 2. The liquid solution is introduced to the line and its vapours are carried using some carrier gas like argon, nitrogen or air. The vapour is carried to an atomizer from which it is sprayed on to the preheated substrate. The quality of these films depends on parameters such

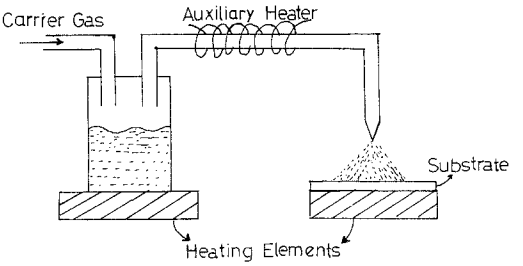

Figure 2 Basic set-up for the spray deposition.

as the spray rate, the substrate temperature, and the ratio of the various constituents in the solutions. In order to obtain films with good conductivity, it is normally essential that complete oxidation of the metal should be avoided. This is generally achieved by adding appropriate reducing agents such as propanol, ethyl alcohol or pyrogallol. This technique has been most widely used [34–50] because it is easy to use and economical. Kulaszewicz *et al.* [34] have grown thin films of doped and undoped In_2O_3 and SnO_2. Antimony-doped films were fabricated using either $SnCl_2$ or $SnCl_4$ with $SbCl_3$ dissolved in water, with 2% pyrogallol. The films of lowest sheet resistivity were observed when 2.5 ml of 2% of pyrogallol was added to 18 ml of mixed $SnCl_2$ and $SbCl_3$ solutions. A sheet resistivity as low as 65 ohm $\square^{-1}$ and 10 ohm $\square^{-1}$ for SnO_2 and In_2O_3 films could be achieved depending upon the quantity of doping and the reducing agent. Manifacier *et al.* [35–37] have reported the fabrication of films of tin-doped In_2O_3 and fluorine-doped SnO_2 films of sheet resistivity ~ 10 ohm $\square^{-1}$ and transmission greater than 85%. An aerosol stream [38] containing an alcoholic solution of $SnCl_4$ and $InCl_3$ was sprayed through a preheating furnace. For doping the SnO_2 films with fluorine, an organo-fluorine compound, trifluoroacetic acid or ammonium fluoride was added and for doping In_2O_3 films with Sn, $SnCl_3 \cdot 5H_2O$ was added. The temperature of the substrate was kept higher than 350° C. The optimum concentration of various ingradients was reported to be (1) fluorine-doped SnO_2: $SnCl_4$: $5H_2O$–0.329, H_2O–0.329, CH_3CH_2OH–0.329, NH_4F–0.013; (2) Sn–In_2O_3: In_2Cl_3–0.0817, H_2O–0.4204, CH_3CH_2OH–0.4204, $SnCl_4 \cdot 5H_2O$–0.0024, HCl–0.0751.

Sanz Maudes and Rodriguez [39] have used this technique to grow undoped and doped SnO_2 films on glass and silicon wafers. The solution used consisted of 32.21 wt % ethanol, 40.35 wt % deionized

water and 27.43 wt% of $SnCl_4$. Doping was achieved by mixing this solution with a hydro-alcoholic solution of 4.20 wt% of $SbCl_3$, 51.53 wt% ethanol, 42.94 wt% of deionized water, and 1.33 wt% HCl. The carrier gas used was nitrogen and the diameter of the nozzle of the sprayer was 0.5 mm. The films grown on substrates at temperatures below 623 K were amorphous and others grown at higher substrate temperatures were polycrystalline. Shanthi *et al.* [40, 41] have more recently used this technique to grow undoped and antimony-doped SnO_2 films. The typical spray mixture used consisted of 0.7 M $SnCl_4$, 10 M propanol and 0.2 M HCl with varying concentrations of $SbCl_3$. The pH of the solution was ~0.5. The temperature of the substrate was kept between 340 to 540° C. Compressed air at a pressure of ~0.5 kg cm^{-2} was used as a carrier gas and the spray rate was ~10 $cm^3 min^{-1}$. The films produced were polycrystalline and the quality of the films improved when the substrate temperature was increased. The optimum concentration of antimony was estimated to be 3 mol% and the resistivity of the films were ~ 3×10^{-3} ohm cm. Ma [42] and Ortiz [43] have grown the films of cadmium stannate using spray pyrolysis techniques. The starting solution [43] consisted of 0.1 M $SnCl_4$ and 0.2 M $CdCl_2$ and the pH of the solution was adjusted to 1.5 with HCl, to obtain a complete dissolution of $SnCl_4$. The substrate temperature was varied from 370 to 450° C and the flow rate of the nitrogen gas from 8.2 to 10.9 l min^{-1}. The solution flow rates were 1.5 to 2.1 $cm^3 min^{-1}$. The films produced were polycrystalline and the sheet resistivity and transmission were ~400 ohm $\square^{-1}$ and 83% respectively.

Kulaszewicz [45] has described a slightly different type of apparatus which consists of a rotating sprayer having a swinging motion. More homogeneous and reproducible results were obtained. Recently Pommier *et al.* [46] have modified the spray technique to grow films of uniform thickness over a larger surface area (10 cm × 10 cm). The nozzle moved in the $X-Y$ directions above the substrate which was preheated to higher temperatures. The solution was pulverized by means of a neutral gas (nitrogen) so that it arrived at the substrate in the form of very fine drops under optimal condition. Indium–tin oxide layers with resistivity ~ 2×10^{-4} ohm cm and transmission ~92% were achieved.

2.3. Vacuum evaporation

Though this is one of the most commonly used methods for growing thin films of various semiconductor materials it has not so far been used extensively for growing thin transparent conducting coatings. The basic set-up is shown in Fig. 3. An oil diffusion pump equipped with a liquid nitrogen trap can be used to attain a base pressure ~ 10^{-6} torr. A resistively heated tungsten or tantalum source, or an electron-beam heated source, can be used to evaporate the charge. The substrate heater is placed above the substrate to heat it to the required temperature. Oxygen or an argon–oxygen mixture can be admitted through the calibrated leak valve. These oxide materials can be evaporated in two ways: (i) by evaporating metal-oxide, e.g. SnO_2, In_2O_3, Cd_2SnO_4, or (ii) by evaporating the metal in the presence of oxygen. It has often been observed that when oxide materials are evaporated as such there is always some deficiency of oxygen in the films. Either the films must be evaporated in the partial pressure of oxygen or some post-deposition heat treatment in air is essential to achieve good quality films. This method has been used by a few workers [51–60] using either resistive heating or electron beam heating. Pan and Ma [53] evaporated thin films of indium oxide from In_2O_3 powder. The partial pressure of the oxygen was achieved by first creating a vacuum ~ 1×10^{-6} torr and then introducing oxygen such that the pressure increased to the range ~ 8×10^{-5} to 2×10^{-4} torr. The substrate temperature

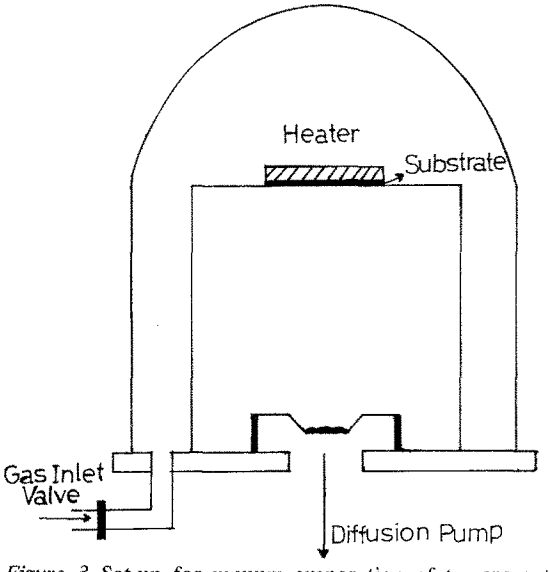

Figure 3 Set-up for vacuum evaporation of transparent conducting thin films.

was kept at around 320 to 350° C and the evaporation rate ~1.5 to 3 nm min^{-1}. It was observed that an addition of about 5 to 20% of metallic tin in In_2O_3 charge improved the properties significantly and reproducible results on conductivity ~10^4 ohm^{-1} cm^{-1} and tramsmission ~90% could be achieved. Mizuhashi [54] used this technique to grow indium–tin oxide films. In_2O_3 and SnO_2 were evaporated from different crucibles. The amount of SnO_2 into the films was adjusted by adjusting the rates of evaporation of SnO_2 and In_2O_3. The partial pressure of the oxygen was ~10^{-4} torr. The lowest resistivity found for indium tin oxide films was 2×10^{-4} ohm cm with a carrier density of ~10^{21} cm^{-3} and a mobility ~30 $cm^2 V^{-1} sec^{-1}$ at the optimized doping level ~5 wt% and substrate temperature 400° C. Noguchi and Sakata [55] have reported the growth of films of In_2O_3 by evaporating indium metal of "five nines" purity in vacuum at a partial pressure of oxygen ~1×10^{-3} torr. The substrate temperature was in the range of 200 to 500° C and the deposition rate was ~0.3 nm sec^{-1}. The transparency (~75%) in these films were slightly poor as compared to the films grown using other techniques. However, the conductivity was fairly good (~2 to 3×10^3 ohm^{-1} cm^{-1}). Nath and Bunshah [56] have further improved this technique for fabricating high quality films of In_2O_3 and indium-tin oxide. They evaporated the metallic tin or tin–indium alloy in the presence of Ar–15% O_2 gas mixture. In order to enhance the reactivity of indium or In–Sn vapour species with the reaction gas, a dense plasma was generated by employing a thoriated tungsten emitter and a low voltage anode assembly. Magnetic field coils were also used to confine the plasma and to enhance the reaction further. Sheet resistivity as low as 2.2 ohm $\square^{-1}$ and transmission as high as 96% were achieved using this technique.

2.4. Sputtering techniques

2.4.1. d.c. and r.f. sputtering

These are the most commonly used when device quality films are required. Sputtered films of metal oxides like the evaporated ones, tend to be deficient in oxygen. To remove the deficiency, the films should be sputtered in the presence of oxygen or a post-deposition heat treatment should be given. Fig. 4 shows the basic set-up for sputtering. Typical conditions for d.c. sputtering for these materials are cathode voltage ~1 to 3 kV, cathode

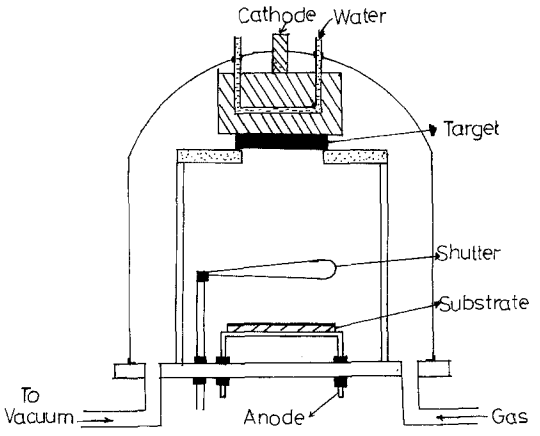

Figure 4 Set-up for the depostion of films using sputtering techniques.

current density = 1. to 3 mA cm^{-2}, cathode–substrate distance = 2 to 4 cm, working gas pressure ~10^{-2} torr. For r.f. sputtering, power ~200 W to 1 kW is delivered to the target from an r.f. generator of 13 MHz via an impedance matching network. Pre-deposition sputtering is essential in order to clean the surface of the target. The films can be fabricated in both ways: (i) sputtering of the metal oxide target, (ii) reactive sputtering of the metal target in the presence of oxygen. Many workers [12, 61–83] have utilized these techniques to grow high quality transparent conducting films. Fan *et al.* [76] investigated the properties of the r.f. sputtered indium tin oxide as a function of the oxygen partial pressure in a mixture with argon. It was observed that the properties were strongly dependent on the oxygen partial pressure. The resistivity of these films was least (~3×10^{-4} ohm cm) for the oxygen partial pressure of about 3×10^{-5} torr and then started increasing again. The transmission, on the other hand reached its maximum value ~90% for a partial pressure of oxygen ~3×10^{-5} torr and was practically constant with further increase of oxygen contents. Leja *et al.* [77] have observed that during the reactive sputtering of tin in the presence of oxygen, the resulting films consisted of various phases of tin, SnO and SnO_2. The presence of these phases was dependent on the oxygen concentration in the mixture of argon and oxygen introduced into the chamber during sputtering. Nojik [66] and Haacke and co-workers [67–69] prepared films of cadmium stannate by r.f. sputtering of the oxide target without using oxygen; and of the Cd–Sn alloy using oxygen. The substrate temperature was raised to 750° C

during the deposition and the deposition rate was $\sim 30\,nm\,min^{-1}$. It was observed that the films grown at a substrate temperature $\sim 300^{\circ}C$ were amorphous but when they were grown at higher substrate temperatures they were crystalline. A significant effect of the post-deposition heat treatment in a hydrogen or argon–CdS atmosphere in improving the conductivity and transmission was observed. On the other hand, Miyata and co-workers [70–74] have reported that the reactive sputtering of a Cd–Sn alloy target produced very good quality cadmium stannate films. The oxygen ratio in the $Ar–O_2$ mixture was raised to optimize the conditions and the deposition rate was ~ 1.5 to $4.5\,nm\,min^{-1}$. Films with minimum resistivity $\sim 2.5 \times 10^{-4}$ ohm cm were obtained with a gas mixture of Ar–6% O_2. These films had an optimal transmission $\sim 90\%$. Miyata *et al.* [75] also fabricated cadmium stannate films by sputtering a sintered $CdO–SnO_2$ target in argon or argon/oxygen atmosphere. Unlike others, these authors were able to grow films of minimum resistivity $\sim 4.8 \times 10^{-4}$ ohm cm and transmission $\sim 85\%$ in pure argon, and found that the addition of oxygen resulted in increase of resistivity and decrease of transmission.

2.4.2. Magnetron sputtering

Conventional diode sputtering sources, whilst offering the simply controlled and reproducible film growth rates desirable for the reactive deposition of coatings, suffer mainly from two disadvantages: (i) the deposition rate is very low, (ii) there is a substantial heating due to target secondary electron bombardment of the substrate. By employing a magnetic field to confine these electrons to a region close to the target surface, the heating effect is substantially reduced and the plasma is intensified, leading to greatly increased deposition rates. Film preparation of the conducting and transparent films of semiconducting oxide materials have been recently tried by magnetron sputtering [84–86]. Buchanan *et al.* [86] have grown films of indium–tin oxide of resistivity as low as 5×10^{-4} ohm cm and transmittance $\sim 85\%$. The substrate temperature was kept $\sim 730^{\circ}C$ and the rate of deposition was $\sim 16\,nm\,min^{-1}$. The authors were able to deposit these films onto a variety of substrates including pyrex, quartz and mylar.

2.4.3. Ion plating

The production of low resistivity coatings normally requires elevated temperatures of the order of 400 to $500^{\circ}C$. An alternative to the supply of energy to the condensing molecules by heating the substrates is to provide it by the simultaneous bombardment of the surface with high energy active molecules, then reactive processes can be encouraged on the substrate surface. The process where these particles are provided from a discharge running in the residual gas in the vacuum chamber has become known as ion-plating. Since the substrate temperatures involved are very low, this process can be used to coat in plastic materials, and it can be introduced into almost all the sputtering processes. This technique has recently been used by many workers [87–93]. Howson *et al.* [87, 88] have used a reactive ion plating process to grow coatings of the oxides of indium and indium tin alloys starting from the metal sources. A radio freqeuncy discharge of 13.56 MHz was used to create a discharge in the residual atmosphere of argon/oxygen. The amount of energy put into the substrate from the discharge was found to be best characterized by the d.c. negative standing valtage that appeared on that electrode as a result of ion and electron current balancing during the r.f. discharge. Films of conductivity $\sim 5 \times 10^{2}\,ohm^{-1}\,cm^{-1}$ were achieved when the r.f. bias was such that the maximum negative voltage was ~ 500 volts. Machet *et al.* [89] have used resistance heated vapour sources to deposit indium tin oxide. Indium and tin were separately evaporated in oxygen and the rate of evaporation of the individual elements was adjusted to have the desired value of tin contents in indium oxide. The substrate temperature was ~ 300 to $350^{\circ}C$ and the growth rate was ~ 4 to $6\,\mu m\,h^{-1}$. Under optimum conditions the films had a resistivity $\sim 10^{-3}$ ohm cm and transmission $\sim 85\%$. Fluorine-doped In_2O_3 films were also produced by Avaritsiotis and Howson [90] using this technique. The fluorine was introduced as a gaseous dopant in In_2O_3 by evaporating the metal in an oxygen–CF_4 r.f. discharge. It was observed that the incorporation of 2.3 at % fluorine in the films induced a sheet resistivity of 40 ohm $\square^{-1}$ and a transmittance of 80%. Recently Ridge *et al.* [91] have used this technique to coat continuously a flexible plastic sheet with indium tin oxide. A magnetron sputtering source was modified to accommodate this reactive tin-plating process. By controlling the sputtering rate precisely ($\sim 10\,nm\,min^{-1}$) and the partial pressure of oxygen

($\sim 0.9 \times 10^{-3}$ torr), they were able to achieve highly transparent ($\sim 90\%$) and reasonably good conducting (~ 400 ohm $\square^{-1}$) films.

2.4.4. Ion-beam sputtering

Since ion-beam sputtering, unlike r.f. sputtering, involves minimal intrinsic heating and electron bombardment, so the effect on the substrate is minimized. High quality films of transparent conducting oxides have recently been fabricated by this technique [81, 94] at deposition temperatures less than 100° C. Fan [94] has used an argon-ion beam source with a typical value of current of 50 mA. The electrical and optical properties of the films were found to depend on the oxygen partial pressure. The films had an electrical resistivity ($\sim 5.5 \times 10^{-4}$ ohm cm) and transparency $> 78\%$ at oxygen pressure of 2 to 3×10^{-5} torr, both on glass and mylar substrates.

In addition to these techniques, a few workers have used other techniques, e.g. glow discharge [95] and the Pyrosol process [96]. But these processes have not been widely used.

2.5. Electrical properties

The electrical properties of these oxide materials depend strongly on the deposition parameters, the presence of impurities, post-deposition annealing and the presence of oxygen during fabrication. The effect of various parameters on the electrical properties are discussed briefly in the following sections. The data cited here for discussion is just representative all that has been published.

2.5.1. Effect of oxygen

Fig. 5 shows typical results of films of indium tin oxide [86] prepared by magnetron sputtering, as a function of oxygen partial pressure. The films were prepared from the In_2O_3 target containing 9 mol% SnO_2. The system was first pumped down to 1×10^{-7} torr, and the required oxygen partial pressure was introduced in argon at an overall sputtering pressure of $\sim 4 \times 10^{-3}$ torr. It can be observed from this diagram that there exists a broad minimum in the resistivity corresponding to an oxygen pressure of 2.7×10^{-5} torr. The observed initial slight decrease in resistivity is because the addition of oxygen enhances crystallization of the films. Similar enhanced crystallization with added oxygen has also been reported for amorphous films of non-oxide semiconductors [97]. Though the mechanism is not yet understood, most probably the oxygen concentration affects the growth pattern and the film prefers to crystallize. The observed high carrier concentration at low values of added oxygen and the decrease in carrier concentration with increasing added oxygen suggests that the free carrier concentration results from oxygen vacancies [11, 13, 14].

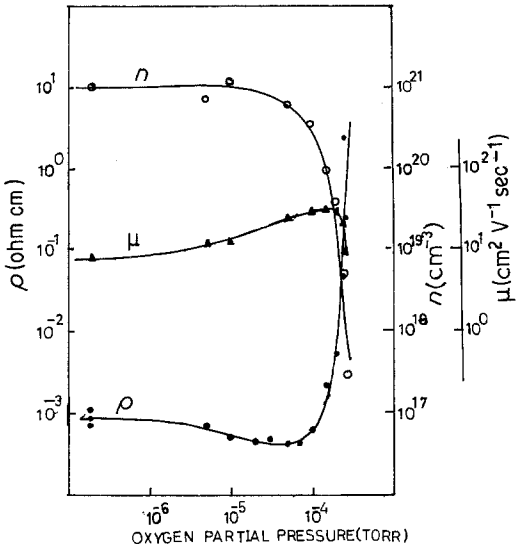

Figure 5 Effect of oxygen on the electrical properties of indium tin oxide films [86].

Fig. 6 gives typical results for the films of cadmium stannate [73] as a function of oxygen concentration. The films were prepared under a total pressure of 3×10^{-2} torr using the sputtering technique in an argon–oxygen atmosphere. For the oxygen concentration in an argon–oxygen atmosphere of 2%, the resistivity is about 10 ohm cm.

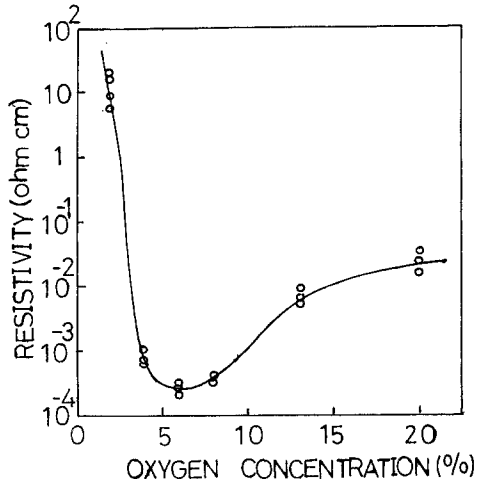

Figure 6 Effect of oxygen on the electrical properties of cadmium stannate films [98].

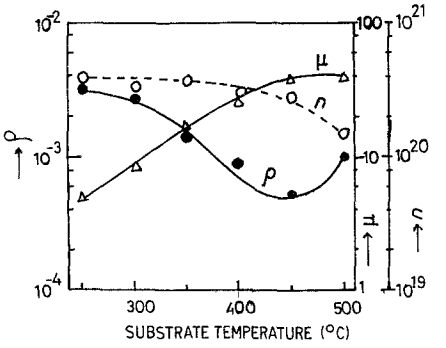

Figure 7 Effect of substrate temperature on the electrical properties of In_2O_3 films [54].

With increasing oxygen concentrations, the resistivity decreases to a minimum of 2.5×10^{-4} ohm cm at 6% oxygen concentration. The resistivity starts increasing again with further increase of oxygen; at 20% oxygen concentration, the average resistivity is about 2×10^{-2} ohm cm, two orders of magnitude higher than the minimum value.

In order to have the films of lowest resistivity, the concentration of oxygen has to be adjusted to an optimum value.

2.5.2. Effect of substrate temperature

Figs. 7, 8 and 9 show typical results for the electrical properties of In_2O_3 [54], SnO_2 [40] and Cd_2SnO_4 [43] as a function of substrate temperature. It can be observed from these figures that the resistivity decreases at first and then increases again as the substrate temperature is increased. On the other hand, the carrier concentration first either remains practically constant or increases with the increase of substrate temperature; and then starts decreasing with the further increase of substrate temperature. The decrease in electron concentration at higher substrate temperatures

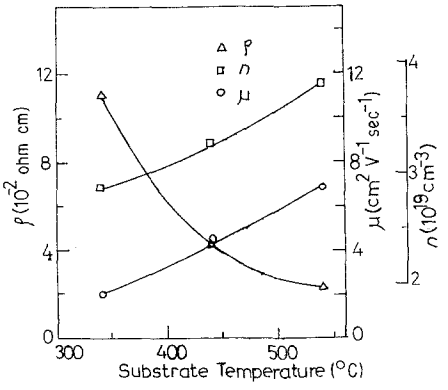

Figure 8 Effect of substrate temperature on the electrical properties of SnO_2 films [40].

further confirms that the free carrier concentration is mainly because of oxygen vacancies, as suggested by Fan and Goodenough [13] and Bosnell and Waghorne [11]. The initial increase in carrier concentration in these films with substrate temperature is because the crystallite size improves significantly, thus reducing the grain boundary scattering mechanism. This is related to the carrier concentration as

$$n = n_0 e^{-q\phi/kT} \quad (1)$$

where n is the carrier concentration for a film having a grain boundary potential barrier of ϕ at any temperature T, n_0 is the carrier concentration in the absence of grain boundaries, k is Boltzmann's constant and q is the electronic charge.

The observed initial increase in conductivity in these figures can also be understood on the same reasoning that the crystallite size as well as the crystalline nature of these films improves with the increase of substrate temperature thus resulting in increase in mobility and conductivity.

2.5.3. Effect of impurities

Impurities have been found to affect the electrical properties appreciably. Figs. 10 and 11 show typical variation of the electrical parameters of indium oxide films doped with tin [36] and fluorine [90] respectively. It can be observed from these figures that initially the concentration of free carriers increases with the increase of the tin/indium or fluorine/indium ratio, whereas further increase of these elements affects the electrical properties adversely. The initial increase may be explained on the basis that tin and fluorine act as substitutional impurities and replace indium and oxygen respectively in order to give donor electrons. Since the observed carrier concentration is quite large ($\sim 10^{21}$ cm^{-3}), it indicates that there is significant contribution from oxygen vacancies and interstitial indium atoms, in addition to the substitutional tin or fluorine ions. The mobility decreases gradually and the carrier density decreases very fast for dopant concentrations greater than the optimum value. This can be explained as follows: the addition of tin or fluorine liberates a great many carriers at first but further addition inevitably causes disorders in the In_2O_3 lattice. Disorder enhances the scattering mechanism such as phonon scattering and ionized impurity scattering, resulting in decrease in mobility. A crystal lattice distorted too much in

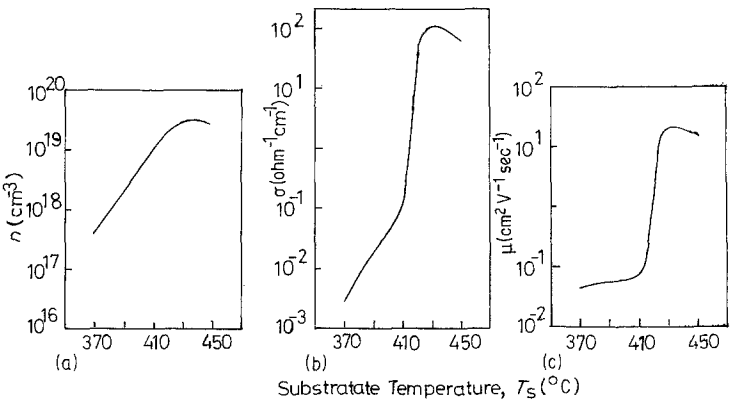

Figure 9 Effect of substrate temperature on the electrical properties of Cd_2SnO_4 films [43].

this way can no longer be effective either in generating Sn^{4+} ions on the substitutional sites of In^{3+} or in generating oxygen vacancies. It may, however, be mentioned that the optimum value of tin or fluorine in In_2O_3 may vary slightly depending on the fabrication procedure.

Fig. 12 shows the effect of the impurity concentration of antimony [40] on the electrical transport properties of SnO_2 films. The resistivity decreases up to a concentration of 3 mol% and starts increasing for higher antimony concentrations. The carrier concentration, however, shows a steep increase initially up to 6 mol% and a gradual decrease thereafter. The results can be understood on the following basis.

On addition of antimony up to 6 mol% the carrier concentration increases since antimony forms a shallow donor level [98]. However for higher values of antimony concentration there is a decrease in both the carrier concentration and the mobility. This is probably because a large addition of antimony distorts the lattice, and increases the activation energy of the donor. It can be further observed from this figure that the value of mobility increases initially up to ~1.4 mol% antimony and then starts decreasing. The initial increase in mobility is due to the increase in grain size from 25 nm for undoped films to 60 nm for 1.4 mol% antimony-doped films, which reduces the grain boundary scattering contribution significantly. The decrease in mobility beyond this value of concentration of antimony can be attributed to the increase in contribution from ionized impurity scattering.

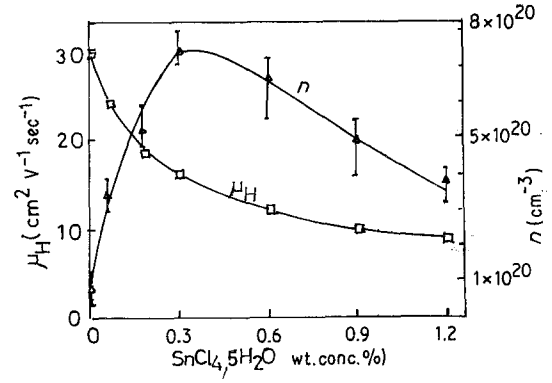

Figure 10 Effect of tin doping on the electrical properties of In_2O_3 film [36].

2.5.4. Scattering mechanisms

The scattering mechanism involved in the conduction process in these films are little understood explanations. Whatever are available, they are diverse. Shanthi *et al.* [40] have indicated that the mobility of SnO_2 and antimony-doped SnO_2 films increases with the increase of temperature in the temperature range 200 to 300 K. The authors have attributed their results to the presence of grain boundary scattering. The results have been analysed in accordance with the Petritz model [99], according to which

$$\mu_H = AT^{-1/2} \exp\left(\frac{-q\phi}{kT}\right) \qquad (2)$$

where μ_H is the observed mobility and A is constant depending upon the deposition conditions. According to this relation $\log \mu_H T^{1/2}$ against $1/T$ should give the value of ϕ. Such a plot has been drawn by Shanthi *et al.* [40] and the value of ϕ has been estimated to be about 30 meV. Dewall and Simonis [100] on the other hand have reported that the mobility of undoped and fluorine-doped SnO_2 films decreases with the increase of temperature in the temperature range 0 to 300° C. The observed decrease in mobility with temperature is probably because of the predominance of lattice scattering in their films.

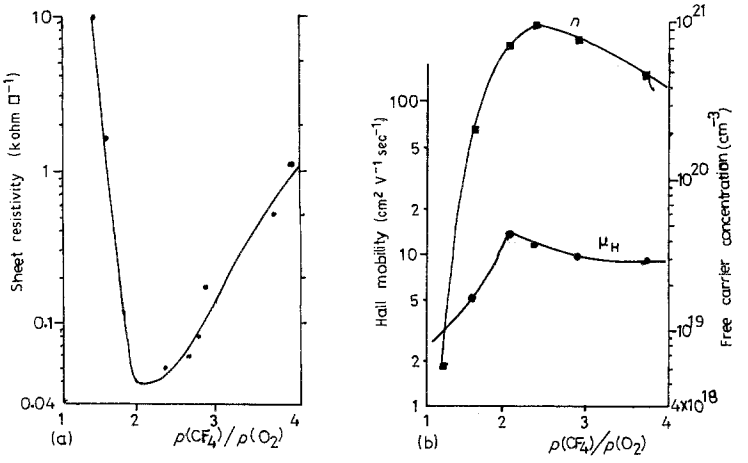

Figure 11 Effect of fluorine doping on the electrical properties of In_2O_3 films [90].

Noguchi and Sakata [55, 101] have reported that the mobility observed in films of In_2O_3 and tin-doped In_2O_3 is practically independent of temperature (in the temperature range 77 to 300 K). The mobility, however, is a strong function of carrier concentration, approximately in accordance with the relation $\mu_H \propto n^{3/2}$. These results have been analysed in the light of Johnson and Lark-Horovitz's theory [102] of ionized scattering for degenerate semiconductors.

Looking at the importance of these oxide materials, much work is still needed to understand fully the scattering mechanisms.

2.6 Optical properties

Optical properties of thin conducting transparent films also depend on deposition parameters, the presence of oxygen, impurities, carrier concentration, etc. The effect of these parameters on optical properties is discussed briefly in the following text.

2.6.1. Effect of oxygen

The optical properties of these films are not as sensitive to the presence of oxygen as the electrical properties. Fig. 13 shows the transmission of indium–tin oxide films [81] as a function of oxygen partial pressure for ion-beam sputtered films. It can be observed from this diagram that the transmission increases rapidly at first, exceeding 80% at 3×10^{-5} torr, and then becomes almost constant at about 90%. Clearly, the presence of oxygen beyond a certain limit is ineffective in controlling the optical properties of these films. However, the electrical properties depend strongly on the oxygen partial pressure and therefore in order

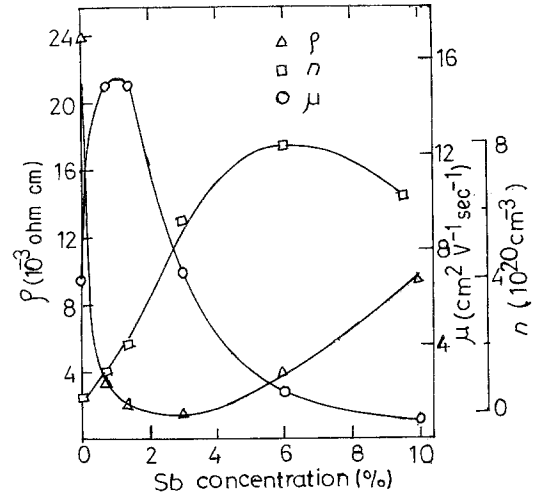

Figure 12 Effect of antimony doping on the electrical properties of SnO_2 films [40].

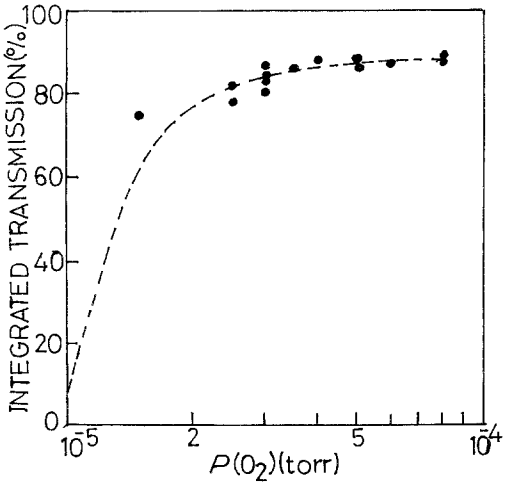

Figure 13 Effect of oxygen on the transmission of indium tin oxide films [81].

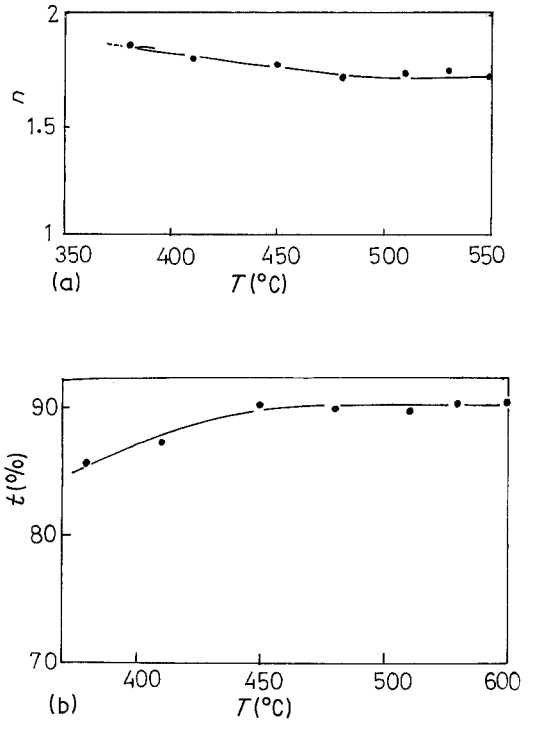

Figure 14 Effect of substrate temperature T on the refractive index n and transmission t of indium–tin oxide films [46].

to have high quality films, the value of oxygen partial pressure is critical.

2.6.2. Effect of substrate temperature

Fig. 14 shows the effect of substrate temperature T on the refractive index N and the transmission t for indium–tin oxide films prepared by the spray technique [46]. The refractive index decreases significantly with increase of substrate temperature. On the other hand, the value of transmission increases with increase of temperature up to a substrate temperature ~450°C and then becomes practically independent of substrate temperature at higher temperatures. It has been suggested that this dependence on substrate temperature, is because films grown at a lower substrate temperature have a higher degree of surface roughness, which causes light scattering and thus reduces the transmission.

2.6.3. Reflection and transmission properties

Figs. 15, 16 and 17 show typical variations of transmission and reflection of In_2O_3 [54], SnO_2 [96] and Cd_2SnO_4 [103] films. It can be seen that the films are transparent in the visible region and

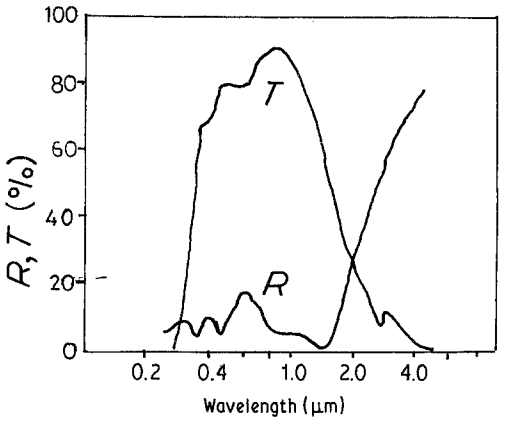

Figure 15 Reflection and transmission properties of In_2O_3 films [54].

are highly reflecting in the infrared region. The wavelength at which the reflection becomes prominent, known as plasma wavelength, depends strongly on the carrier concentration. The transmission decreases with increase of free carrier concentration, whereas the reflectivity increases with increase of carrier concentration. The plasma reflection edge shifts to shorter wavelengths with increase of carrier concentration. This property of reflection in the infrared and transmission in the visible can be understood on the basis of classical theory:

$$\epsilon' = N^2 - K^2 = \epsilon_L - \omega_n^2/(\omega^2 + \gamma^2) \quad (3)$$

$$\epsilon'' = 2NK = \frac{\gamma}{\omega}\frac{\omega_n^2}{(\omega^2 + \gamma^2)} \quad (4)$$

where ϵ' and ϵ'' are the real and imaginary parts of the dielectric constant, K is the extinction coefficient and ϵ_L is the dielectric constant of the material in the absence of free electrons. The wavelength λ is related to ω by the relation $\lambda = 2\pi C_0/\omega$ where C_0 is the velocity of light. ω_n and γ are correlated with the free carrier concentration n and the mobility μ of the charge carriers by the equations

$$\omega_n = \frac{ne^2}{\epsilon_0 m_e} \qquad \gamma = \frac{em_e}{\mu}. \quad (5)$$

ϵ_0 is the permittivity of free space and m_e is the effective mass of the free carriers.

The material properties change drastically when ϵ' passes through $\epsilon' = 0$. This defines the cut-off wavelength of the filter, where metal-like infrared reflection changes to dielectric-like visual transmission. It is called the plasma wavelength of the free electron material and is given by

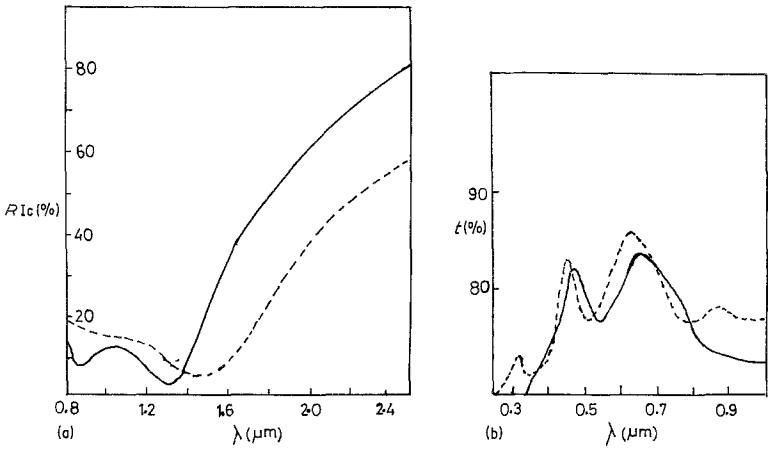

Figure 16 Reflection and transmission properties of SnO_2 films [96]. (a) fluorine-doped SnO_2 (F/Sn = 25%; — d = 60 nm; - - - d = 400 nm). (b) SnO_2 ——, d = 450 nm; SnO_2/SiO_2, - - -, d = 350 nm.

$$\lambda_p = 2\pi C_0 \left(\frac{ne^2}{\epsilon_0 \epsilon_L m_e - \gamma^2} \right)^{-1/2} . \quad (6)$$

Since the value of γ is quite small and thus can be neglected, the cut-off wavelength λ_p can be adjusted simply by changing the carrier concentration of the films by doping.

Knowing the values of the plasma wavelength, one can find out the value of the effective mass of the carriers as a function of carrier concentration. Such calculations have been made by Ohhata *et al.* [104] and Shanthi *et al.* [40] for In_2O_3 and SnO_2 films respectively. The variation of effective mass with carrier concentration is shown in Figs. 18 and 19. Such large changes in effective mass with carrier concentration indicates non-parabolicity of the conduction band.

2.6.4. Optical absorption studies

The optical absorption studies [14, 16, 22, 40, 104, 105] in thin films indicate that there are both direct and indirect allowed transitions present in accordance with the realtions $\alpha \approx (h\nu - E_g)^{1/2}$ for direct transitions, and $\alpha \approx (h\nu - E_g')^2$ for indirect allowed transitions, where $h\nu$ is the energy of the photons, α is the absorption, and E_g and E_g' are the energy gaps for these two transitions. Different values of E_g and E_g' have observed by different workers depending upon the deposition conditions. The range of values observed for SnO_2, In_2O_3 and Cd_2SnO_4 are given in Table I. The values of the energy gaps are also a function of the carrier concentration and it has been observed that the absorption edge shifts towards higher energy with an increase in the carrier concentration. This is known as the Burstein–Moss shift [106, 107]. Assuming that both the conduction band and the valence band are parabolic, the energy shift can be given in the same way as the free energy of a free electron gas:

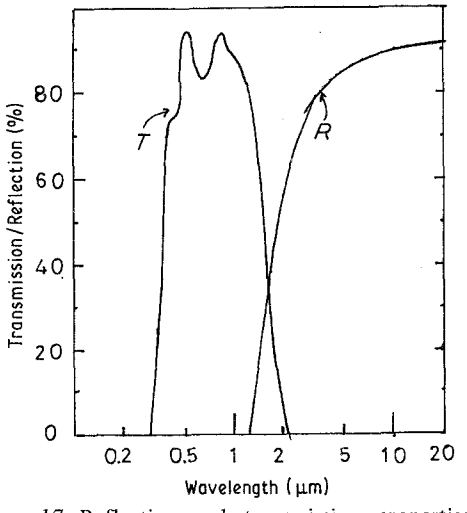

Figure 17 Reflection and transmission properties of Cd_2SnO_4 films [103].

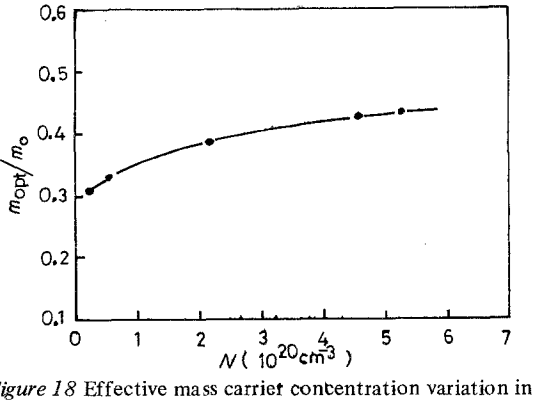

Figure 18 Effective mass carriet concentration variation in In_2O_3 films [104].

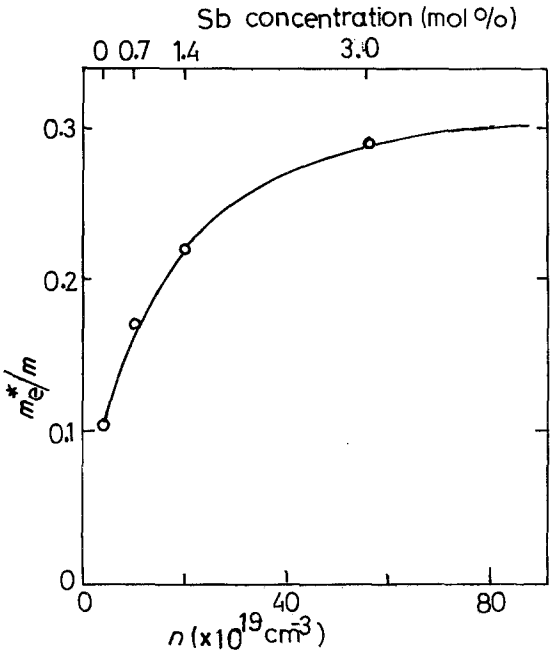

Figure 19 Effective mass carrier concentration variation in SnO_2 films [40].

$$E_g - E_{g0} = \frac{\hbar}{2m_{vc}}(3\pi^2 n)^{2/3} \quad (7)$$

where E_{g0} is the intrinsic band gap and m_{vc} is the reduced mass defined by $1/m_{vc} = 1/m_c + 1/m_v$ where m_c and m_v are the effective masses in the conduction band and valence band respectively, and $\hbar = h/2\pi$ where h is Planck's constant. This relationship indicates that the shift should be proportional to $n^{2/3}$, and the coefficient should lead to the value of m_{vc}. Such a linear dependence of the shift on $n^{2/3}$ has been observed by many workers. Representative data for In_2O_3 are shown in Fig. 20 [104].

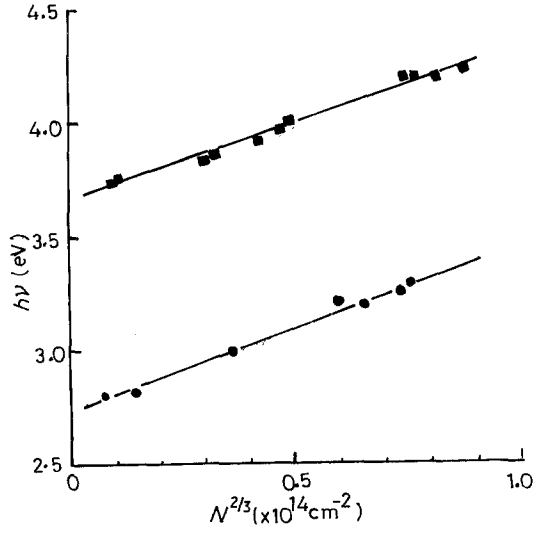

Figure 20 The effect of carrier concentration on the band edge shift for In_2O_3 [104]. ▪ direct allowed transition d = 142.5 to 145 nm; • indirect allowed transition d = 473 to 500 nm.

2.7. Figure of merit

Common to all transparent conductor applications is the need for optimizing the electrical and optical coating parameters. Depending on the type of device requiring a transparent electrode, the optical transmission and the electrical conduction of the electrodes should exceed certain minimum values. Ideally both the parameters should be as large as possible but their inter-relationship usually excludes the simultaneous achievement of both these criteria. In order to compare the performance of various transparent conductors, the most widely used figure of merit is defined as [108]

$$\phi_{TC} = \frac{T^{10}}{R_S} \quad (8)$$

where T is the transmission and R_S is the sheet resistance. The maximum value of the thickness that corresponds to this figure of merit is given by

$$t_{max} = 1/10\alpha \quad (9)$$

where α is the optical absorption coefficient.

Table II compares the values of ϕ_{TC} for different films prepared by different techniques.

3. Applications of transparent conducting films

3.1. Transparent heat-reflecting films

Wavelength-selective surfaces have many important applications, especially in solar energy conversion. There are basically two classes of wavelength selective surfaces: selective black absorbers and transparent heat mirrors. Selective black absorbers absorb solar radiation and have a low infrared thermal emissivity. Such absorbers are generally prepared by coating a metal of high infrared reflectivity with a thin film that is transparent in the infrared but highly absorbing in the visible. Such a film can be prepared by depositing a thin layer of semiconductor having an energy gap of about 1 eV together with an antireflection coating [112]. The other method of preparing selective black absorbers is to use cermet films, e.g. MgO–Au [81, 113, 114], and Cr_2O_3–Cr [115, 116]. The other type of wavelength-selective surfaces, transparent heat

TABLE II Comparison of properties of conducting transparent films prepared by different techniques

Material	Process	Sheet resistance, R_S (ohm $\square^{-1}$)	Transmission T (%)	Figure of merit, ϕ_{TC} (ohm^{-1})	Mobility ($cm^2 V^{-1} sec^{-1}$)	Carrier concentration (cm^{-3})	Reference
In_2O_3	Evaporation	88	80	1.2202×10^{-3}	72	3×10^{20}	[54]
In_2O_3:Sn	Evporation	8	90	4.3585×10^{-2}	30	$\sim 10^{21}$	[54]
In_2O_3 + In	Evaporation	6.75	91	5.7691×10^{-2}	70	4.5×10^{20}	[53]
In_2O_3:Sn	Spray	3.1	88	8.9839×10^{-2}	–	–	[36]
SnO_2:F	Spray	10.6	86	2.0878×10^{-2}	–	–	[36]
Cd_2SnO_4	Spray	400	83	3.8790×10^{-4}	20	2.9×10^{19}	[43]
SnO_2:Sb	Spray	160	90	2.1792×10^{-3}	–	–	[45]
SnO_2:Sb	Spray	86	84	2.0337×10^{-3}	12	8×10^{20}	[40]
Indium tin oxide (ITO)	Spray	4	90	8.717×10^{-2}	50	6×10^{20}	[46]
SnO_2:Sb	CVD	72	87	3.4503×10^{-3}	–	–	[109]
In_2O_3:Sn	CVD	3	75	1.8771×10^{-2}	–	–	[109]
Cd_2SnO_4	Sputtering	2.4	83	6.4650×10^{-2}	–	–	[108]
Cd_2SnO_4	Sputtering	14	93	3.4570×10^{-2}	22	5×10^{20}	[75]
Cd_2SnO_4	Sputtering	6.6	90	5.2830×10^{-2}	–	6×10^{20}	[98]
Cd_2SnO_4	Sputtering	1.35	90	2.5828×10^{-1}	10–40	$\sim 10^{20}$	[69]
Cd_2SnO_4	Sputtering	2.4	82	5.7270×10^{-2}	–	–	[67]
In_2O_3:Sn	Sputtering	5	90	6.9736×10^{-2}	35	7×10^{20}	[76]
ITO	Ion beam sputtering	6	84	2.9150×10^{-2}	30	4×10^{20}	[94]
ITO	Magnetron sputtering	6.6	85	2.9829×10^{-2}	12	10^{21}	[86]
ITO	Magnetron sputtering	40	90	8.7170×10^{-3}	–	–	[110]
ITO	Ion plating	10	80	1.0737×10^{-2}	40	3×10^{20}	[87]
In_2O_3:F	Ion plating	40	80	2.6844×10^{-3}	13	7×10^{20}	[90]
In_2O_3:Sn	Activated reactive evaporation	20	90	1.7434×10^{-2}	20–30	10^{21}	[111]

mirrors, are surfaces which have a high reflectance for the parts of the wavelength spectrum which are described as heat, and consequently they have a low emissivity for these wavelengths. These surfaces are produced by two different techniques: (1) by the use of multilayers of dielectrics and interference effects to give the required properties, and (2) by the use of intrinsic optical properties of surfaces of bulk conductors. The optical properties of conducting materials are characterized by a plasma frequency for their free carriers. The material shows a reflectance that falls from dielectric behaviour to near-zero and then rises to near unity with increasing wavelength. In the region of dielectric behaviour, the material is transparent and the lower wavelength limit of transparency is governed by interband absorption. Optical properties due to free carriers within semiconductors can lead, therefore, to regions of transparency between the plasma frequency and the frequency corresponding to the onset of interband absorption. Metals may also be used as transparent heat mirrors if their interband absorption is sufficiently small to allow a film to be thick enough to be coherent whilst remaining transparent. Metals such as gold, silver and copper, which possess a relatively high transmission in the visible range of the spectrum and a relatively high coefficient of reflection in the longer wavelength region, have proved effective. To improve the transparency in the visible range, additional interference layers of high refractive index materials are used. The most commonly used coatings [117, 118] are ZnS/Au/ZnS, TiO_2/Au or Ag or Cu/TiO_2, Bi_2O_2/Au, or Ag or Cu/Bi_2O_3, ITO/Au or Ag or Cu/ITO. Fig. 21 shows typical results [117] of the transmission as a function of wavelength for various layer combinations in which the metallic layer is embedded between two transparent layers of metallic oxide of appropriate thickness.

Another simple technique to achieve the same goal is to coat the surface with doped or undoped In_2O_3, SnO_2 or Cd_2SnO_4, or their mixed oxides, of suitable carrier concentration. Many workers [44, 81, 85, 119–123] have reported the use of these coatings for heat reflecting applications. In order to have low emissivity, the sheet resistivity of the films should be less than 20 ohm $\square^{-1}$. A typical curve depicting this is shown in Fig. 22, for In_2O_3 films [121], in which the value of emissivity is given for different values of sheet resistivity. The samples were heated to 80° C and the emissivity was measured under roughly normal incidence with a broad-band detector. Dewall and Simonis [100] have estimated that for an optimum transparent heat mirror based on SnO_2 coatings, a high electron mobility of at least 40 $cm^2V^{-1}sec^{-1}$ and an electron concentration of about 3×10^{20} cm^{-3} are required. With the techniques described in the earlier section, it seems quite feasible to achieve such properties.

This property has also been exploited and used in low pressure gas discharge lamps [107, 124], solar collectors [103, 116, 121, 125, 126] and incandescent lamps [81].

3.2. Heterojunction solar cells

There has been considerable interest in recent years directed towards the development of conducting oxide silicon solar cells. These heterojunction solar cells offer the possibility of fabrication of solar cells with performance characteristics suitable for large scale terrestial applications. Such an interest is also based on the fact that these

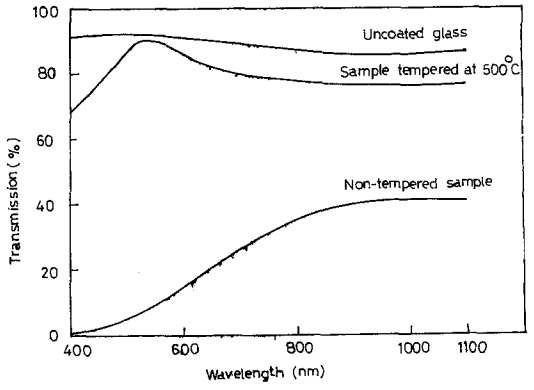

Figure 21 Transmission as a function of wavelength for various layer combinations [117].

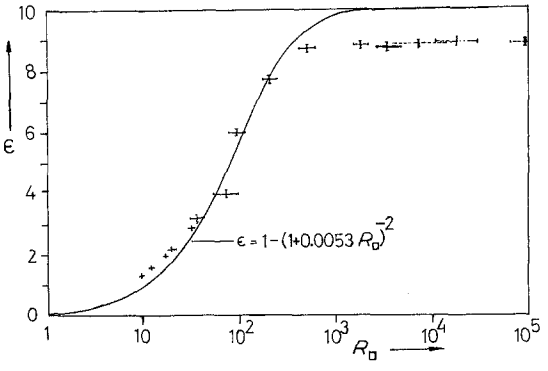

Figure 22 The effect of sheet resistivity on the emissivity of In_2O_3 films [121].

heterojunction devices have a number of advantages over diffused p–n junction silicon cells and have the potential for lower cost fabrication. Some of the advantages are: (a) ease of fabrication of the junction because of lower junction formation temperatures; (b) the conducting transparent film permits the transmission of solar radiation directly to the active region with little or no attenuation, so that solar cells based on these materials result in improved sensitivity in the high-photon-energy portion of the solar spectrum; and (c) these films can serve simultaneously as a low resistance contact to the junction and as an antireflection coating for the active region. The refractive index of the film, N_f, is related to the refractive index N_S of the substrate by the relation $N_f = (N_S)^{1/2}$, for an antireflection coating. The refractive indices of indium–tin oxide and silicon, which are ~2 and 4 respectively satisfy this condition well.

In addition, the lower processing temperature is especially suited for polycrystalline silicon since preferential diffusion along grain boundaries can be avoided. Moreover, the deposition techniques are consistent with high yield and fast throughput processing, thus avoiding degradation of semiconductor minority carrier properties and suggesting a compatibility with film and polycrystalline substrates [127, 128]. Fig. 23 shows the typical configuration [129] of a cell based on silicon substrates. The single crystal or a polycrystalline substrate wafer is polished. Prior to deposition of SnO_2 or In_2O_3, the wafer is chemically etched in a $HF–HNO_3$ mixture. The thickness of the film is usually kept ~ 100 nm in order to give the desired antireflection properties. After the deposition of SnO_2 back contact metallization is accomplished by vacuum depositing 100 nm of titanium followed by 500 nm of silver. The front-metal grid electrode is formed by sequentially evaporating 100 nm of titanium and 1000 nm of silver through the metal mask. Heterojunction solar cells with a conducting transparent film on silicon, indium phosphide, cadmium telluride, gallium arsenide, etc. have been reported by many workers [127–153].

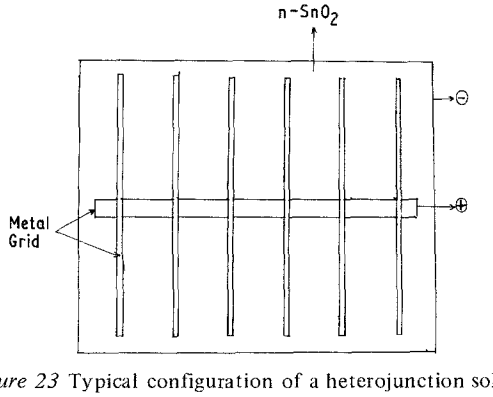

Figure 23 Typical configuration of a heterojunction solar cell [129].

There has also been considerable interest recently in solar cells incorporating an amorphous interfacial layer between the cell substrate and the window [154–157]. The purpose of using this layer is to increase the open-circuit voltage by decreasing the dark saturation current. This semiconductor–insulator–semiconductor (SIS) structure is potentially more stable and theoretically more efficient than either a Schottky or a metal–insulator–semiconductor (MIS) structure. The origins of this potential superiority are the suppression of majority carrier tunnelling in the SIS structure, the absence of thin metal which absorbs light and is subjected to environmental degradation and the wide choice of conductivity and band gaps allowed in the top layer. Table III lists the results of some of the workers on heterojunction solar cells in which the conducting transparent layer has been fabricated using different techniques.

3.3. Gas sensors

Semiconductor materials whose conductance is modulated directly by interaction with an active gas have been studied for many years. There is reversible chemisorption of reactive gases at the surfaces of certain metal oxides and chalcogenides which is accompanied by reversible changes in conductance [164–176]. The recent emergence of concern over pollution; over efficiency in a variety of combustion processes; and over heightened requirements involving poisoning gases has stimulated substantial research and development in the field of semiconductor gas sensors. Most of the sensors used so far are based on doped or undoped tin oxide. Windischmann and Mark [169] have described a thin film SnO_2 sensor for carbon monoxide. The sensors were fabricated by sputtering a hot-pressed SnO_2 target in the presence of oxygen. The film thickness was of the order of 50 nm. The films were tested in a flowing gas system with sensors thermally biased at 200 to 500° C. It was observed that the sensor ceased to work beyond this temperature range. The sensors were tested to detect carbon monoxide in the presence of back-

TABLE III Comparison of solar cell properties based on conducting transparent layers produced by different techniques

Structure	Method of preparation or conducting film	Efficeincy (%)	Reference
SnO_2/Si	Spray deposition	12.3	[129]
SnO_2/Si	Spray deposition	7.2	[149]
SnO_2/Si	Sputtering	12.5	[158]
ITO/Si	Sputtering	13.0	[159]
In_2O_3/Si	Vacuum evaporation	6.0	[160]
ITO/Si	Sputtering	12.0	[159]
ITO/Si	Spray deposition	9.0	[161]
In_2O_3/InP	Sputtering	9.3	[144]
SnO_2/InP	Sputtering	2.2	[144]
ITO/CdTe	Sputtering	8.0	[139]
ITO/InP	Sputtering	14.0	[146]
ITO/InP	Ion-beam sputtering	14.4	[162]
ITO/InP	Magnetron sputtering	9.4	[146]
ITO/GaAs	Magnetron sputtering	1.9	[146]
ITO/GaAs	Ion beam sputtering	5.0	[146]
ITO/GaAs	Sputtering	2.0	[146]
ITO/SiO_x/Si	Spray deposition	11.5	[154]
ITO/SiO_x/Si	Ion beam sputtering	11.9	[163]

ground gas constituents which comprised 10% oxygen, 3% water, 500 ppm sulphur dioxide, 150 ppm nitrogen oxide, 9% carbon dioxide, and the balance nitrogen. Within this range, it was observed that the conductance of the sensor increased with partial pressure P_{CO} of carbon monoxide in the ambient gas according to the relation

$$G = G_0 + \beta(P_{CO})^{1/2} \quad (10)$$

where G_0 is the background conductance in the absence of carbon monoxide and β is a constant. An example of this behaviour is shown in Fig. 24 [169]. The results have been analysed on the basis of the following model. (a) There is a surface reaction between associatively adsorbed carbon monoxide from the ambient gas with chemisorbed oxygen to produce CO_2^-. (b) This is followed by the return of the electron from the CO_2^- to the conduction band, owing to the exothermic reaction energy of the CO oxidation. (c) There is subsequent thermal desorption of the neutral sorbed CO_2. It has also been observed that the speed of response of the sensors increased with the increase of carbon monoxide concentration.

The detectors based on SnO_2 doped with thorium oxide (ThO_2), show the presence of an oscillation phenomenon [171, 172] when the devices are exposed to carbon monoxide gas in air. Since this oscillation phenomenon is absent in the presence of other gases except carbon monoxide, the device can be used to detect carbon monoxide in air. Recently it has been observed [173] that when sensors based on SnO_2-doped with palladium, rhodium or MgO are tested in air, the oscillation phenomenon exists only when hydrogen gas is present in the air. This suggests the possibility of using these devices for sensing hydrogen in atmospheres containing various gases. Nitta *et al.* [170] have reported the fabrication of a propane gas detector using SnO_2 doped with niobium, vanadium, titanium or molybdenum. It was observed that the detectors based on SnO_2 doped with transition metals were relatively more reliable and sensitive for the detection of propane gas.

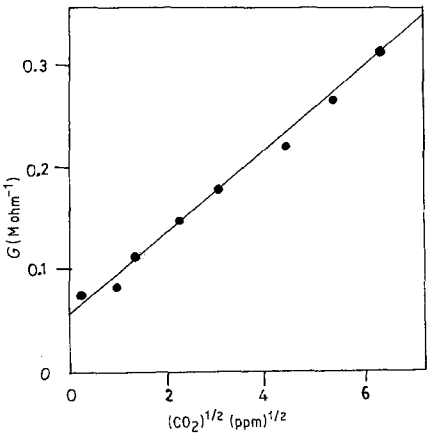

Figure 24 Effect of CO partial pressure on the conductance of SnO_2 films [169].

3.4. Protective coatings

In recent years, increasing demands are being placed on the serviceability of articles fabricated from glass or plastics. Specifically for glass containers, high production speed, lighter weight containers as well as increased bottle-line filling speeds are calling for improved methods to maintain the inherently high strengths of moulded glass surfaces. It is well established now [1, 31, 177–181] that metal oxides and organic coatings have to be applied to glass containers to protect them from frictive damage thereby maintaining a high percentage of pristine strength. These coatings lower the coefficient of friction of the glass surface facilitating the movement of containers through high speed filling lines. The application of tin oxide is made when the containers are hot (~ 400 to 500° C), and the process is normally known as hot end treatment. The containers are consecutively treated with an insoluble coating such as emulsified polyethylene when the containers are at much lower temperatures (100 to 150° C) and the process is referred to as cold end treatment. It has been reported that such treatments produce scuff-free surfaces. Fig. 25 shows the typical values of the friction coefficient of the bottles with and without hot end coatings [178]. The value of the friction coefficient F was in the range 0.8 to 0.9 for uncoated glass-to-glass contacts. Bottles receiving a commercial organic lubricant only, i.e. cold end coating, showed an initial value of F as 0.45 for dry conditions. This value initially decreased rapidly to 0.3 but on repeated frictive testing, it rose to a constant value of about 0.8, indicating that glass to glass contact occurred. Any lubricating qualities, initially present, were either worn away or the organic coating had been cut through by the repeated contact. For only the tin oxide coatings, i.e. hot end treatment the intial value of F was 0.38, and it remained constant for 50 tests. When both tin oxide and organic libricants were applied to glass surfaces, the initial value of F was 0.03 and it remained constant over the repeated tests, demonstrating that the tin oxide coatings act to bond the organic coating more firmly to the glass surface than when no tin oxide is present.

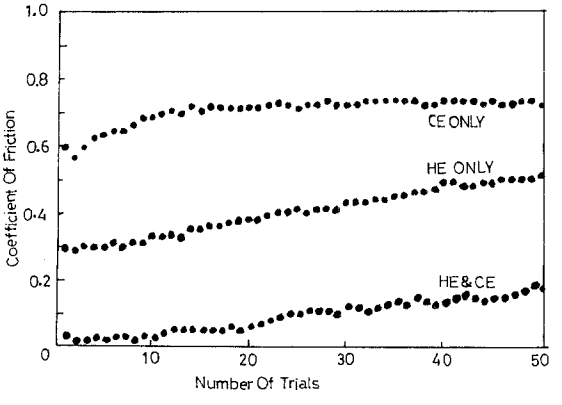

Figure 25 Effect of various treatments on the friction coefficient of bottles as a function of repeated tests [178].

Budd [179] has indicated that these properties of tin oxide coatings are very much related to the level of tin treatment of these bottles. The higher the level of tin, the greater is the resistance to scuffing. It was also observed that the coating of SnO_2 and the organic treatment produced good abrasion resistance and lubricity in the surfaces, which could be maintained through at least 20 alkaline washings of 2.5% NaOH solutions at 65° C. Various set-ups for coatings of SnO_2 on such a large scale has been discussed by many workers [31, 180, 181].

3.5. High power laser applications [5]

Electro-optic shutters based on the longitudinal Pockels effect are required in high energy solid-state systems for fusion research to suppress target-damaging amplified spontaneous emission and to protect the system from target retroreflections. The Pockels cells now used consist of cylindrical KDP crystals with a metal ring around the crystal near the parallel faces. To achieve adequate electric field uniformity over the aperture requires a crystal length-to-diameter ratio of $\geqslant 1.1$. Such crystals with a clear aperture of 5 cm and even somewhat larger are available, but difficult to grow and expensive. A transparent conductive film electrode over the crystal aperture eliminates the length to diameter constraint. The disc crystals can, therefore, be used for the same purpose, provided they are coated with transparent conducting films which can withstand high laser powers. It has been reported by Pawlewicz *et al.* [5] that the r.f. sputtered coatings of $In_{1.9}Sn_{0.1}O_3$ on fused silica exhibited damage thresholds of 2.2 and 3.1 J cm^{-2} for 0.15 and 1 nsec neodymium–glass laser pulses respectively. The thresholds were measured using linearly polarized 1.06 μm pulses, incident on the films at 56° from the normal. The beam diameter was ~ 2 mm. It has also been observed that the damage thresholds did not increase with the square

root of pulse durations, indicating that linear absorption was the cause of damage.

3.6. Space applications [7]

A growing concern about non-uniform electric charge build-up on the exterior surfaces of orbitting satellites has prompted investigations with the preparation and properties of electrically conducting transparent coatings for use as surface layers on temperature control coatings. Field intensity fluctuations in the earth's magnetosphere especially at geosynchronous orbital altitudes continuously irradiated with UV and charged particle radiation may differentially bias spacecraft areas to potentials as high as 10^4V [182]. Spacecraft elements charged to potential differences of this magnitude may perturb the electromagnetic field and charged particle environment that they were launched to measure and may also cause catastrophic failure of operature of operating functions due to spontaneous discharges. Electrical conducting transparent coatings can therefore ensure potential uniformity on the exterior of the satellites. The films should satisfy two conditions: (1) they should be highly conducting, and (2) they should have little effect on the properties of the underlying surfaces even after extended exposures to space environment with charged particles. Hass and his coworkers [7, 138] have shown that In_2O_3 and ITO coatings were well suited for the purpose and the coated surfaces were shown to have excellent stability when exposed to combined UV and charged particle irradiation in both laboratory and actual space flight experiments.

References

1. R. PUYANE (ed.), "Battele Seminar on Coatings on glass, Geneva, Switzerland" September 18–20 1980. *Proc. in Thin Solid Films* **77** (1981) Nos. 1, 2 and 3.
2. H. YOSHIDA, H. FURUBAYASHI, Y. INOUE and T. TONOMURA, *J. Vac. Soc. Jpn.* **19** (1976) 13.
3. J. P. FILLARD and J. C. MANIFACIER, *Jp. J. Appl. Phys.* **9** (1970) 1012.
4. C. TATSUJAMA and S. ICHIMURA, *ibid.* **14** (1976) 843.
5. W. T. PAWLEWICZ, I. B. MANN, W. H. LOWDERMILK and D. MILAM, *Appl. Phys. Lett.* **34** (1979) 196.
6. H. T. TIEN and J. HIGGINS, *J. Electron. Soc.* **127** (1980) 1475.
7. G. HASS, J. B. HEANEY and A. R. TOFT, *Appl. Opt.* **18** (1979) 1488.
8. R. TUETA and M. BRAGUIER, *Thin Solid Films* **80** (1981) 143.
9. C. A. VINCENT, *J. Electron Soc.* **119** (1972) 515.
10. H. KOSTLIN, R. JOST and W. LEMS, *Phys. Status Solidi (a)* **29** (1975) 87.
11. J. R. BOSNELL and R. WAGHORNE, *Thin Solid Films* **15** (1973) 141.
12. J. C. C. FAN and F. J. BACHNER, *J. Electron. Soc.* **122** (1975) 1719.
13. J. C. C. FAN and J. B. GOODENOUGH, *J. Appl. Phys.* **48** (1977) 3524.
14. J. L. VOSSEN, *Phys. Thin Films* **9** (1977) 1.
15. G. HAACKE, *Ann. Rev. Mater. Sci.* **7** (1977) 73.
16. Z. N. JARZEBSKI, *Phys. Status Solidi (a)* **71** (1982) 13.
17. R. G. LIVERSEY, E. LYFORD and H. MOORE, *J. Phys. E* **1** (1968) 947.
18. K. AKIYOSHI, K. YAMAMOTO and H. YOSHIKAWA, Japanese Patent 72, 14, 593 (1972).
19. L. A. RYABOVA and Ya. S. SAVITSKAYA, *Thin Solid Films* **2** (1968) 142.
20. J. A. ABOAF, V. C. MARCOTTE and N. J. CHOU, *J. Electrochem. Soc.* **120** (1973) 701.
21. J. KANE, US Patent 3 854 992 (1974).
22. Z. M. JARZEBSKI and J. P. MORTON, *J. Electro. chem. Soc.* **123** (1976) 199C, 229C, 333C.
23. G. N. ADVANI, A. G. JORDON, Ch. P. LUPIS and R. L. LONGINI, *Thin Solid Films* **62** (1979) 361.
24. E. KAWAMATE and K. OHSHIMA, *Jp. J. Appl. Phys.* **18** (1979) 205.
25. J. KANE, H. P. SCHWEIZER and W. KERN, *J. Electrochem. Soc.* **122** (1975) 1144.
26. J. KANE, H. P. SCHWEIZER and W. KERN, *ibid.* **123** (1976) 269,
27. B. J. BALIGA and S. K. GANDHI, *ibid.* **123** (1976) 941.
28. Y. S. HSU and S. K. GANDHI, *ibid.* **126** (1979) 1434.
29. S. K. GANDHI, R. SIVIY and J. M. BORREGO, *Appl. Phys. Lett.* **34** (1979) 833.
30. O. TABATA, T. TANAKA, M. WASEDA and K. KINUHARA, *Surf. Sci.* **86** (1979) 230.
31. J. M. BLOCHER Jr, *Thin Solid Films* **77** (1981) 51.
32. R. KALBSKOPF, *ibid.* **77** (1981) 65.
33. *J. Less Common Met.* **63** (1979) 111.
34. S. KULASZEWICZ, I. LASOCKA and Cz. MICHALSKI, *Thin Solid Films* **55** (1978) 283.
35. J. C. MANIFACIER, L. SZEPESSY, J. F. BRESSE, M. PEROTIN and R. STUCK, *Mater. Res. Bull.* **14** (1979) 109.
36. *Idem, ibid.* **14** (1979) 163.
37. J. C. MANIFACIAR, J. P. FILLARD and J. M. BIND, *Thin Solid Films* **77** (1981) 67.
38. J. C. MANIFACIER, M. DE MURCIA and J. P. FILLARD, *Mater. Res. Bull.* **10** (1975) 1215.
39. J. SANZ MAUDES and T. RODRIGUEZ, *Thin Solid Films* **69** (1980) 183.
40. E. SHANTHI, V. DUTTA, A. BANERJEE and K. L. CHOPRA, *J. Appl. Phys.* **51** (1980) 6243.
41. E. SHANTHI, A. BANERJEE, V. DUTTA and K. L. CHOPRA, *Thin Solid Films* **71** (1980) 237.
42. Y. Y. MA, *J. Electrochem. Soc.* **124** (1977) 1430.

43. A. ORTIZ, *J. Vac. Sci. Technol.* **20** (1982) 7.
44. O. P. AGNIHOTRI and B. K. GUPTA, in Proceedings of the International Symposium and Workshop on Solar Energy, Part I, Cairo, June 1978 (Pergamon, Oxford, 1980) p. 540.
45. S. KULASZEWICZ, *Thin Solid Films* **74** (1980) 211.
46. R. POMMIER, C. GRIL and J. MARUCCHI, *ibid.* **77** (1981) 91.
47. B. DOGIL, F. FROISSART and A. J. HORODECKI, *J. Phys. D, Appl. Phys.* **12** (1979) 919.
48. T. NAGATOMO and O. OMOTO, *Oyo Buturi (Japan)* **47** (1978) 618.
49. J. C. MANIFACIER, *Thin Solid Films* **90** (1982) 297.
50. P. GROSSE, F. J. SCHMITTE, G. FRANK and H. KOSTLIN, *ibid.* **90** (1982) 309.
51. T. FENG, A. K. GHOSH and C. FISHMAN, *Appl. Phys. Lett.* **34** (1979) 198.
52. C. A. PAN and T. P. MA, *J. Electron. Mater.* **10** (1981) 43.
53. *Idem, Appl. Phys. Lett.* **37** (1981) 163.
54. M. MIZUHASHI, *Thin Solid Films* **70** (1980) 91.
55. NOGUCHI and SAKATA, *J. Phys. D. Appl. Phys.* **13** (1980) 1129.
56. P. NATH and R. F. BUNSHAH, *Thin Solid Films* **69** (1980) 63.
57. N. RUCKER and K. J. BECKER, *ibid.* **53** (1978) 163.
58. D. LASER, *ibid.* **90** (1982) 317.
59. M. MIZUHASHI, *ibid.* **76** (1981) 97.
60. K. B. SUNDARAM and G. K. BHAGAVAT, *Phys. Status Solidi (a)* **63** (1981) K15.
61. A. G. SABNIS and L. D. FEISEL, *J. Vac. Sci. Technol.* **14** (1977) 685.
62. *Idem, IEEE Trans. Parts, Hybrids, Packing* **PHP-12** (1976) 357.
63. A. G. SABNIS and K. Y. CHANG, *Electron. Lett.* **13** (1977) 113.
64. A. G. SABNIS and A. G. MOLDORAN, *Appl. Phys. Lett.* **33** (1978) 885.
65. D. B. FRASER AND H. D. COOK, *J. Electrochem. Soc.* **119** (1972) 1368.
66. A. J. NOJIK, *Phys. Rev.* **B6** (1976) 453.
67. G. HAACKE, *Appl. Phys. Lett.* **28** (1976) 622.
68. *Idem, Thin Solid Films* **55** (1978) 55.
69. G. HAACKE, W. E. MEALMAKER and L. A. SIEGEL, *ibid* **55** (1978) 67.
70. N. MIYATA and K. MIYAKE, *Jpn. J. Appl. Phys.* **17** (1978) 1693.
71. N. MIYATA, K. MIYAKE and S. NAO, *Thin Solid Films* **58** (1979) 385.
72. N. MIYATA and K. MIYAKE, *Surf. Sci.* **86** (1979) 384.
73. N. MIYATA, K. MIYAKE and Y. YAMAGUCHI, *Appl. Phys. Lett.* **37** (1980) 180.
74. N. MIYATA, K. MIYAKE, T. FUKUSHIMA and K. KOGA, *ibid.* **35** (1979) 542.
75. N. MIYATA, K. MIYAKE, K. KOGA and T. FUKUSHIMA, *J. Electrochem. Soc.* **127** (1980) 918.
76. J. C. C. FAN, F. J. BACHNER and G. H. FOLEY, *Appl. Phys. Lett.* **31** (1977) 773.
77. E. LEJA, J. KORECKI, K. KROP and K. TOLL, *Thin Solid Films* **59** (1979) 147.
78. K. B. KAGANOVICH, V. D. OVSJANNIKOV and S. V. SVECHNIKOV, *ibid.* **60** (1979) 335.
79. R. R. MEHTA and S. F. VOGEL, *J. Electrochem. Soc.* **119** (1972) 753.
80. J. A. THORNTON and V. L. HEDGCOTH, *J. Vac. Sci. Technol* **13** (1976) 117.
81. J. C. C. FAN, *Thin Solid Films* **80** (1981) 125.
82. A. G. SABINIS, *Electron. Components Sci Technol.* **7** (1980) 19.
83. V. HOFFMAN, *Opt. Spectra* **12** (1978) 60.
84. K. SUZUKI, M. MIZUHASI, H. SAKATA, *J. Vac. Soc. Jpn.* **21** (1978) 158.
85. R. P. HOWSON and M. I. RIDGE, *Thin Solid Films* **77** (1981) 119.
86. M. BUCHANAN, J. B. WEBLE and D. F. WILLIAMS, *Appl. Phys. Lett.* **37** (1980) 213.
87. R. P. HOWSON, J. N. AVARTSIOTIS, M. I. RIDGE and C. A. BISHOP, *ibid* **35** (1979) 161.
88. *Idem, Thin Solid Films* **58** (1979) 379.
89. J. MACHET, J. GUILLE, P. SAULNIER and S. ROBERT, *ibid.* **80** (1981) 149.
90. J. N. AVARITSIOTIS and R. P. HOWSON, *ibid.* **80** (1981) 63.
91. M. I. RIDGE, M. STENLAKE, R. P. HOWSON and C. A. BISHOP, *ibid.* **80** (1981) 31.
92. J. N. AVARITIOTIS and R. P. HOWSON, *ibid.* **77** (1981) 351.
93. M. M. KUTUZOV, V. V. KOTOV, V. V. KRYACHKO and V. F. SYNOROV, *Inorg. Mater.* **13** (1977) 1616.
94. J. C. C. FAN, *Appl. Phys. Lett.* **34** (1979) 515.
95. D. E. CARLSON, *J. Electrochem. Soc.* **122** (1975) 1334.
96. G. GLANDENT, M. COURT and Y. LAGARDE, *Thin Solid Films* **77** (1981) 81.
97. J. B. WEBLE and D. E. BRODIE, *Cand. J. Phys.* **51** (1973) 493.
98. A. ROHATGI, T. R. VIVERITO and L. H. SLACK, *J. Amer. Ceram. Soc.* **57** (1974) 278.
99. R. L. PETRITZ, *Phys. Rev.* **104** (1956) 1508.
100. H. DEWALL and F. SIMONIS, *Thin Solid Films* **77** (1981) 253.
101. S. NOGUCHI and H. SAKATA, *J. Phys. D, Appl. Phys.* **14** (1981) 1523.
102. V. A. JOHNSON and K. LARK-HOROVITZ, *Phys. Rev.* **71** (1947) 374.
103. G. HAACKE, *Appl. Phys. Lett.* **30** (1977) 380.
104. D. Y. OHHATA, F. SHINOKI and S. YOSHIDA, *Thin Solid Films* **59** (1979) 255.
105. K. B. SUNDARAM and G. K. BHAGAVAT, *J. Phys. D, Appl. Phys.* **14** (1981) 921.
106. E. BURSTEIN. *Phys. Rev.* **93** (1954) 632.
107. T. S. MOSS, *Proc. Phys. Soc. Lond. Soc. B* **67** (1954) 775.
108. G. HAACKE, *J. Appl. Phys.* **47** (1976) 4086.
109. J. KANE and H. P. SWEITZER, *Thin Solid Films* **29** (1975) 155.
110. J. F. SMITH, A. J. ARONSON, D. CHEN and W. H. CLASS, *ibid.* **72** (1980) 469.

111. P. NATH, R. F. BUNSHAH, B. M. BOSOL and O. M. STAFFSUD, *Thin Solid Films* **72** (1980) 463.
112. B. O. SERAPHIN and A. B. MEINDEL in "Optical Properties of Solids – New Developments" edited by B. O. Seraphin (North Holland, Amsterdam, 1976) p. 927.
113. J. C. C. FAN and V. E. HENRICH, *J. Appl. Phys.* **45** (1974) 3742.
114. J. C. C. FAN and P. M. ZAVRACKY, *Appl. Phys. Lett.* **29** (1976) 478.
115. J. C. C. FAN and S. A. SPURA, *ibid.* **30** (1977) 511.
116. J. C. C. FAN and F. J. BACHNER, *Appl. Opt.* **15** (1976) 1012.
117. G. KIENEL, *Thin Solid Films* **77** (1981) 213.
118. J. C. C. FAN, F. J. BACHNER, G. H. FOLEY and P. M. ZARRACKY, *Appl. Phys. Lett.* **25** (1974) 693.
119. R. P. HOWSON, J. N. AVARITSIOTIS, M. I. RIDGE and C. A. BISHOP, *Thin Solid Films* **63** (1979) 163.
120. F. SIMONIS, M. LEIJ and C. J. HOOGENDOORN, *Sol. Energy Mater.* **1** (1979) 221.
121. G. FRANK, E. KAUER and H. KOSTLIN, *Thin Solid Films* **77** (1981) 107.
122. H. DISLICH and E. HUSSMANN, *ibid.* 77 (1981) 129.
123. H. KOSTLIN, *Philips Tech. Rev.* **34** (1974) 272.
124. H. HORSTER, R. KERSTEN and F. MAHDJURI, *Klima und Kalte Ingenieur* **3** (1976) 113.
125. J. SPITZ, *Thin Solid Films* **45** (1977) 34.
126. B. O. SERAPHIN, *Topics Appl. Phys.* **31** (1979) 5.
127. G. CHEEK, N. INOUE, S. GOODNICK, A. GENIS, C. WILMSEN and J. B. DUBOW, *Appl. Phys. Lett.* **33** (1978) 643.
128. T. MIZRAH and D. ADLER, *IEEE Trans. Electron. Devices* **ED-24** (1977) 458.
129. F. FENG, A. K. GHOSH and C. FISHMAN, *Appl. Phys. Lett.* **35** (1979) 266.
130. S. FRANZ, G. KANT and R. L. ANDERSON, *J. Electron Mater.* **6** (1977) 107.
131. W. G. THOMPSON, S. L. FRANZ, R. L. ANDERSON, *IEEE Trans. Electron. Devices* **ED-24** (1977) 463.
132. T. R. NASH and R. L. ANDERSON, *ibid.* **ED-24** (1977) 468.
133. E. Y. WANG and L. HSU, *J. Electrochem. Soc.* **125** (1978) 1328.
134. T. NAGATOMO and O. OMOTO, *Jpn. J. Appl. Phys.* **15** (1976) 199.
135. R. L. ANDERSON, *Appl. Phys. Lett.* **27** (1975) 691.
136. T. NISHINO and Y. HAMAKAWA, *Jpn. J. Appl. Phys.* **9** (1970) 1085.
137. H. MATSUNAMI, K. OO, H. ITO and T. TANAKA, *ibid.* **14** (1975) 915.
138. K. ITO and T. NAKAZAWA, *Surf. Sci.* **86** (1979) 492.
139. F. G. COURREGES, A. L. FAHRENBRUCH and R. H. BUBE, *J. Appl. Phys.* **51** (1980) 2175.
140. J. SCHEWCHUN, D. BURK and M. B. SPITZER, *IEEE Trans. Electron Devices* **ED-27** (1980) 705.
141. G. CHEEK, A. GENIS, J. B. DUBOW and V. R. PAI VERNEKER, *Appl. Phys. Lett.* **35** (1979) 495.
142. J. CALDERER, J. C. MANIFACIER, L. SZEPESSY, J. M. DAROLLES, and M. PEROTIN, *Rev. Phys. Appl.* **14** (1979) 485.
143. P. SMITH, R. SINGH and J. DUBOW, *J. Appl. Phys.* **51** (1980) 2164.
144. M. J. TSAI, A. L. FAHRENBRUCH and R. H. BUBE, *J. Appl. Phys.* **51** (1980) 2696.
145. C. FISHMAN, A. K. GHOSH and T. FENG, *Sol. Energy Mater.* **1** (1979) 181.
146. K. G. BACHMANN, H. SCHREIBER, Jr, W. R. SINCLAIR, P. H. SCHMIDT, F. A. THIEL, E. G. SPENCER, G. PASTEUR, W. L. FELDMANN and K. SREEHARSHA, *J. Appl. Phys.* **50** (1979) 3441.
147. G. K. BHAGAVAT and K. B. SUNDARAM, *Thin Solid Films* **63** (1979) 197.
148. I. CHAMBOULEYRON and E. SAUCEDO, *Sol. Energy Mater.* **1** (1979) 299.
149. T. NAGATOMO, M. ENDO and O. OMOTO, *Jpn. J. Appl. Phys.* **18** (1979) 1103.
150. A. K. GHOSH, C. FISHMAN and T. FENG, *J. Appl. Phys.* **50** (1979) 3454.
151. H. TAKAKURA, M. S. CHOE and Y. HAMEKAWA, *Jpn. J. Appl. Phys. Suppl.* **19** (1980) 61.
152. K. ITO and T. NAKAZAWA, *Trans. Inst. Electron. Commun. Eng. Jpn. Sect. E* **E63** (1980) 485.
153. J. MURAYAMA, K. KAWAJIRI, Y. MIZOBUCHI and Y. NAKAJIMA, *Jpn. J. Appl. Phys. Suppl.* **19** (1980) 127.
154. S. ASHOK, P. P. SHARMA and S. J. FONASH, *IEEE Trans. Electron. Devices* **ED-27** (1980) 725.
155. J. SHEWCHUN, D. BURK, R. SINGH, M. SPITZER and J. DUBOW, *J. Appl. Phys.* **50** (1979) 6524.
156. J. SHEWCHUN, J. DUBOW, C. W. WILMSEN, R. SINGH, D. BURK and J. F. WAGER, *ibid.* **50** (1979) 2832.
157. A. I. MALIK, V. B. BARANYUK and V. A. MANASSON, *Appl. Sol. Energy* **16** (1980) 1.
158. A. K. GHOSH, C. FISHMAN and T. FENG, *J. Appl. Phys.* **49** (1978) 3490.
159. J. B. DUBOW, D. E. BURK and J. R. SITES, *Appl. Phys. Lett.* **29** (1976) 494.
160. S. W. LAI, S. L. FRENZ, G. KENT, R. L. ANDERSON, J. K. CLIFTON and J. V. MASI, in Proceedings of the 11th IEEE Conference on Photovoltaics Specialists, Scottdale, Arizona, May 1975 (IEEE, New York, 1975) p. 398.
161. J. P. SCHUNCK and A. COCHE, *Appl. Phys. Lett.* **35** (1979) 863.
162. K. SREE HARSHA, K. J. BACHMANN, P. H. SCHMIDT, E. G. SPENCER and F. A. THIEL, *Appl. Phys. Lett.* **30** (1977) 645.
163. A. P. GENIS, P. A. SMITH, K. EMERY, R. SINGH and J. B. DUBOW, *Appl. Phys. Lett.* **37** (1980) 77.
164. W. H. BRATTAIN and J. BARDEEN, *Bell Syst. Technol. J.* **32** (1953) 1.
165. G. A. SOMORJAI, *J. Phys. Chem. Solids* **24** (1963) 175.

166. A. L. ROBINSON and R. H. BUBE, *J. Electrochem. Soc.* **112** (1965) 1002.
167. F. B. MICHELETTI and P. MARK, *Appl. Phys. Lett.* **19** (1967) 136.
168. S. BAIDYAROY and P. MARCK, *Surf. Sci.* **30** (1962) 53.
169. H. WINDISCHMANN and P. MARK. *J. Electrochem. Soc.* **126** (1979) 627.
170. M. NITTA, S. KANEFUSA and M. HAVADOME, *ibid.* **125** (1978) 1676.
171. M. NITTA, S. KANEFUSA, Y. TAKETA and M. HARADOME, *Appl. Phys. Lett.* **32** (1978) 590.
172. M. NITTA and M. HARADOME, *IEEE Trans Electron. Devices* **ED-26** (1979) 219.
173. S. KANEFUSA, M. NITTA and M. HARADOME, *J. Appl. Phys.* **52** (1981) 498.
174. *Idem, ibid.* **50** (1979) 1145.
175. M. NITTA and H. HARADOME, *J. Electron. Mater.* 8 (1979) 571.
176. H. PINK, L. TREITINGER and L. VITE, *Jpn. J. Appl. Phys.* **19** (1980) 513.
177. H. P. WILLIAMS, *Glass Technol.* **16** (1975) 34.
178. R. D. SOUTHWICK, J. S. WASYLYK, G. L. SMAY, J. B. KEPPLE, E. C. SMITH and B. O. AUGUSTSSON, *Thin Solid Films* **77** (1981) 41.
179. S. M. BUDD, *Thin Solid Films* **77** (1981) 13.
180. J. D. J. JACKSON, B. RAND and H. RAWSON, *ibid.* **77** (1981) 5.
181. N. JACKSON and J. FORD, *ibid.* **77** (1981) 23.
182. S. E. DEFOREST, *J. Geophys. Res.* 77 (1972) 651.
183. J. J. TRIOLO, J. B. HEANEY and G. HASS, *SPIE* **121** (1977) 46.

Received 8 April
and accepted 22 April 1983